

AERO-PROPULSIVE CHARACTERIZATION OF A FLIGHT VEHICLE WITH TWO SIDE-JETS

R. Balasubramanian; Jessy Prabhu Dayal; R. Krishnamurthy; Debasis Chakraborty
 Defence Research and Development Laboratory (DRDL)
 Kanchanbagh Post, Hyderabad-500 058
 Email : debasis_cfd@drdl.drdo.in; debasis_drld@yahoo.co.in

Abstract

Numerical simulations were carried out to study the aero-propulsive characteristics of a flight vehicle using the in-house developed Reynolds Averaged Navier-Stokes code CERANS. The analyses involved subsonic external flow with inclined supersonic dual sustainer jets at various angles of attack, roll orientations and side slip. The control characteristics of the configuration are evaluated for the flow with and without sustainer jets. Numerical simulations indicated that the jet plume exhausting out of the scarf sustainer nozzle grazed and clung to the airframe for a considerable downstream distance causing serious damage to the airframe. This numerical study led to an important design change of the sustainer nozzle shape from 'scarf' to 'conical' which alleviated plume interference problem with the airframe.

Keywords: Aero-propulsive Characterization, Dual Side-jets, Sustainer Nozzles, CERANS

Introduction

Mission requirements and operational convenience require the use of side-jets in atmospheric flight vehicles. The side-jets may have significant effect in the vehicle performance as the jet exhaust plume turns over following exit from the nozzle and travels downstream where it can interfere with the vehicle body or aft fins and other control surfaces. Past studies have indicated that this jet/fin interaction can change the pressure field on the fins and alter the forces [15]. The role of Counter-rotating Vortex Pair (CVP) and Horseshoe Vortices (HSV) in the far field of the jet in cross flow interaction is discussed adequately in the literature [6-9]. These vortices are generated as the jet is turned over and realigned by its encounter with the freestream. The strong CVP is believed to be principally responsible for the interaction with downstream fins.

Because of its importance in science and engineering, side jet interaction with free stream is studied extensively for high altitude and high Mach number conditions [10,11] as well as for subsonic Mach numbers [12-18] at sea level conditions. Detailed experimental flow field analysis using PIV measurements were made by Beresh et al. [12-14], for study of penetration of a transverse / inclined supersonic jet into a subsonic compressible crossflow. A supersonic jet interacting with subsonic compressible crossflow

was investigated using both experimental and numerical simulation by Chocinski et al. [15]. The wall shear flow patterns obtained around the side jet nozzle exit from both experiment and computation are compared and discussed. The effect of boundary layer thickness and jet to freestream dynamic pressure ratio on flow field pressure distributions for a supersonic under-expanded jet into a high subsonic crossflow was discussed by Hojaji et al. [16]. Both RANS [17] and LES [18] methodologies were employed to explore experimental condition of Beresh et al. [12-14]. The evaluation of two equation RANS turbulence models for jet-in-crossflow problem [17] has revealed that the predictive capability of this class of two equation model is qualitative. Although LES study [18] has demonstrated the ability to predict the flowfield characteristics, no evaluations of its ability to predict jet/fin interactions are presented. In addition, LES is still too expensive for calculations in a design environment. It is clear that the interaction of supersonic jets in subsonic crossflow require further investigation.

In the present study, an integrated aero-propulsion characterization of flight vehicle, which involves inclined supersonic jet penetration into a subsonic crossflow, is presented using an in-house developed RANS code, CERANS [19-22]. Due to difficulty in performing wind tunnel

experiments with hot jet rocket exhaust, the aerodynamic characterization of the flight vehicle was carried out for jet-off condition. The ground test of sustainer motor firing performed at a quiescent condition cannot bring out the effect of external flow aerodynamics on the overall flow environment. The problem of such complex magnitude needs a sophisticated, integrated aerodynamic, aero-propulsive and the aero-thermal response analyses toolkit and the maturity of current CFD methods can complement the experimental testing. The CFD solution can provide alternate design option to solve the complex problem in a cost effective manner.

The Geometry

The flight vehicle geometry, considered in the present study, consists of a blunt spherical nose-cylinder with cruciform low aspect ratio wings and cruciform fins in-line with the wings as shown in Fig.1. The propulsion system of flight vehicle consists of a booster-cum-sustainer rocket system. The initial boost-thrust is provided by the booster rocket which produces thrust along the axis of the body. The sustainer rocket system is a separate propulsive unit housed ahead of the booster rocket system with its jet-plume exhausted through dual, side-mounted inclined nozzles, which propels the flight vehicle towards the target. Though the thrust vector of the sustainer nozzle is along the inclined nozzle axis, the resultant thrust of the dual nozzles is produced along the body axial direction.

The two diametrically opposite nozzles of the sustainer motor are placed inter-digitized with wings and fins. Two types of sustainer nozzles (1) the scarf nozzle with exit plane flushed along the airframe and (2) the conical nozzle with bump-cum-dimple arrangement are considered in the present study. Two pairs of diagonally opposite wire-tunnels are present at azimuth mid-plane between wing-fin panels which house the two diametrically opposite sustainer nozzles. The booster nozzle is a fixed bell shaped nozzle attached at the base of the core body. As per the present jet exhaust design, the hot and high temperature jet-exhaust gases have to traverse the spatial expanse from the mid-body of the vehicle to tail end till the sustainer rocket burns out completely. This may burn or melt the airframe components downstream. The impingement of hot jet on fins can also cause adverse control behavior and can alter external aerodynamic characteristics as compared to a jet-off scenario.

Analysis

Three dimensional Reynolds Averaged Navier Stokes (RANS) equations are solved along with turbulence model in a hybrid unstructured mesh. The effect of two species interaction are modeled by solving an addition equation of species conservation and airframe material temperatures are estimated by solving one dimensional heat conduction equation. The developed software was validated for number of aerodynamic problems ranging from very low subsonic to hypersonic flows [19-22] and the solver with multi species model is applied to stage separation problem of a strategic launch vehicle [21]. The details of computational grid, flow solvers are presented in the subsequent sections.

Grid Generation

The flight vehicle geometry consists of several surface projections in the form of support pads, bulk heads, casings, wire-tunnels, antennae, launch shoes and the wings and fins. Hence the surface mesh modeling needs to capture the finer details of the geometry for accurate flow simulations. Unstructured hybrid grids were generated around the geometry using a commercial grid generator [23]. The near wall mesh is clustered and extruded with prism layer for numerically resolving the boundary layer. Since the external flow is subsonic, the inflow, farfield and outflow boundaries are positioned at very large distances away from the body (twice the length) so that the influence of near-body flow field at these boundaries are very small. Computational grid around the geometry are carefully constructed with specific, componentwise mesh enrichments. To capture the jet-plumes from the scarf as well as conical nozzles, several, uniform, dense mesh zones of various levels were embedded along the plume-path-trails. The other regions of mesh enrichments include (i) region around the spherical nose (ii) all the protrusions (iii) region around wing-tips and fin-tips and (iv) base regions of core-body as well as booster nozzle. A typical grid in **the pitch plane and at a fin cross sectional plane in Fig.2.**

The near wall spacing for the various grids ranges from about 2 micron to 1mm, with the lowest spacing at the nozzle throat region and the highest spacing at the wing and fin tips. The average near wall spacing over the body varies from about 40 to 100 microns. The near wall Y^+ values ranges from about 0.2 to 150 for the adiabatic flow simulations considered for evaluation of aerodynamic forces and moments. The minimum Y^+ is observed over the mid-body region and around the wing-fin-body junc-



tions. Numerical simulations performed with two grids of sizes 9 million and 12 million cells respectively and the aerodynamic coefficients were found to have very small differences between them (maximum of about 3 to 5%) and the grid independence of the results were established. For the test case involving isothermal wall temperature of 300K, a fine grid consisting of about 14 million cells with highly clustered mesh (0.3 micron) near the jet plume-airframe interaction region is generated. In this case, the minimum Y^+ was observed to be around 0.05 for the body region and the Y^+ in the zone of interest at nozzle exit plane is of order 1.

Flowsolver Details

Fluid Flow Solver (CERANS)

CERANS [19-22] is a three dimensional, finite volume, MPI parallel, implicit RANS flowsolver. It handles the geometry through a preprocessor which generates data structure such that the geometric information is grid-format-independent. The numerical fluxes for the mean flow equations were evaluated using modified **Roes flux** formulae [24] for the convective fluxes and central differencing for the diffusive fluxes. Second order spatial accuracy was used for evaluating the mean flow fluxes and slope limiter was used to preserve monotonicity in regions of discontinuities. One equation Spalart-Allmaras [25] turbulence model addresses the turbulence closure problem. For the present simulations, the global minimum time step is used for time evolution as two different time scales that of the external flow and the jet plume are involved. Convergence is accelerated with Point Jacobi based implicit procedure and the criteria used for convergence is based on asymptotic steady state limit of the aerodynamic coefficients.

Calorically Perfect Equivalent Specie model (CPES)

The external air is considered as perfect gas and hence the gas thermal properties such as ratio of specific heats, gas constant and Prandtl number are assumed invariant. Since, the focus of the present study is mainly on obtaining accurate aerodynamic forces and moments, **and therefore** the gas-dynamic properties are assumed as calorically perfect. For modeling the mixing of air and jet plume with different set of gas thermal properties, the simplest air-plume-jet mixing methodology 'Calorically Perfect Equivalent Specie' model (CPES) [26] is used. An additional equation for conservation of specie-mass for obtain-

ing the specie density is considered and hence the mass fraction of 'equivalent specie' is solved. The values of mixture gas thermal properties are obtained by linear interpolation using the mass fraction of air and plume-jet and are used for modeling the convective transport mixing and the diffusion transport mixing. The conservation of 'equivalent specie' mass equation is discretized in the framework of modified Roe scheme [24] and implemented in the MPI parallel version of CERANS code. Implementation of this model resulted in successful realization of aero-propulsion characterization of flight vehicle with high degree of robustness and accuracy.

Thermal Solver (ATPC)

In order to estimate the material temperature for the airframe subjected to severe thermal loading, the transient heat conduction analysis is performed using an in-house developed Airframe Temperature Prediction Code (ATPC) [27], where the one-dimensional heat conduction equation is solved along the depth of the material from the surface using finite difference method. The details of the 1D numerical discretization for conduction problem with effects of surface radiation follows the work of NASA's TCAT [28]. Multiple stack of material can be considered for conduction analysis along the depth of the airframe thickness. A point implicit method is used for time integration of the governing equations. The ATPC code is applied offline in which the requisite surface heat flux inputs are obtained based on the heat transfer coefficient evaluated using the 'isothermal method' [29]. Details of this method are provided in Section - Results and Discussions. This approach is adequate for plume-airframe interaction problem for obtaining the airframe material temperature.

Boundary Conditions

The flow conditions considered are presented in Table-1.

The characteristic boundary conditions are specified at the inflow, farfield and outflow boundaries. The no slip condition along with an adiabatic wall condition is applied at wall for simulations considered for aerodynamic characterization, whereas the temperature at the wall is specified as 300K for all the isothermal wall simulations. The Dirichlet type jet boundary condition was imposed at the inlet of the nozzle convergent section.

Table-1 : Freestream and Jet Flow Conditions		
Parameter	Air @ Sealevel, Freestream	Jet @ Convergent - Inlet
Mach Number	0.51 and 0.544	0.170
Angle of Attack α (deg)	0 to 20	--
Roll Orientation, ϕ (deg)	-90 to +90	--
Side Slip Angle, β (deg)	2 and 6.6, for specific cases	--
Fin Deflection, δ_{FIN} (deg)	-20, -10, 0, 10 and 20 for all panels	--
Specific Heat Ratio, γ	1.4	1.2
Pressure	0.1 MPa	49.4 MPa
Density	1.1549 Kg/m ³	5.1333 Kg/m ³
Temperature	303.15 K	3073 K
Molecular Viscosity, μ	1.7849e-5 Kg/m-sec	8.15e-5 Kg/m-sec
Prandtl Number, Pr	0.725	0.610
Gas Constant, R	287.15 J/Kg-K	313.16 J/Kg-K

Results and Discussions

For the temporal evolution, a global minimum time step with a CFL number of about 8 to 10 is used. It took about 80 to 150 thousand iterative time steps for the solution to converge. For the simulation without plume-jet (jet-off condition), convergence to steady state was achieved in about 10 to 15 thousand iterations using the local time stepping with a CFL value of 2 to 4. The computed solution in the nozzle is compared with one dimensional nozzle theory and a very good match between the two is observed.

For aerodynamic characterization of flight vehicle with scarf sustainer nozzles, roll angle considered is 45 degrees, indicating 'x' orientation for the wings and fins with the sustainer nozzles contained in the vertical plane (x-z plane). The numbering system for the cruciform wings and fins along with the direction indicating the angle of attack ' α ', roll angle ' ϕ ' and side slip angle ' β ' are depicted in Fig.3.

The Qualitative Flow Feature

The qualitative features of the flow field of scarf nozzle are depicted in Fig.4 through the Mach number distribution at the pitch plane for two different flight conditions; (1) $M_\infty=0.54$, $\alpha=4^\circ$ and (2) $M_\infty=0.54$, $\alpha=4^\circ$. The jet plume issuing out of the scarf nozzle and the resultant trajectory is clearly seen from these contours. Due to the influence

of external flow, the plume for $M_\infty=0.54$ tends to get compressed and bends towards the body; while the plume path for $M_\infty=0.1$ is straight and along the nozzle center-line. As the dynamic pressure is very low for quiescent condition, the external flow could not exert any influence to alter the plume trajectory as it emerges out of the nozzle. At the nozzle exit plane, the jet pressure variation is observed as highly over-expanded at the plume core and under-expansion regions at the corners. The average exit Mach number at the plume core is about 3.20 and the peak is 3.40.

Aerodynamic Characteristics of Flight Vehicle with Scarf Nozzles

The plots of variation of normal force coefficient and with angle of attack are shown in Fig.5. The normal force coefficient shows almost a linear variation with angle of attack. The axial force coefficient is constant for almost all the angles of attack. The side force coefficient is seen to be negligible up to α of 8° and increase further with angle of attack. The center of pressure varies from 5.1D to 6D (where D is the diameter of the flight vehicle) for the entire α range of 0 - 20° .

Simulations are carried out to find the effect of side-slip on the jet-on aerodynamic characteristics. Two simulations that of $\alpha=10^\circ$, $\beta=6.63^\circ$ and $\alpha=11.83^\circ$, $\beta=20^\circ$ corresponding to a resultant angle of attack of 12° , were

performed. For the first case, the jet was observed to impinge on a leeward fin as seen in the density contours at a fin cross-section in Fig.6.

Thermal Problems Posed by the Scarf Nozzle

The plume structure around the scarf nozzle exit plane (shown later in Fig.9) indicate that the jet-plume at the downstream end of the nozzle undergoes a strong compression and further clings and grazes along the airframe wall for a considerable distance downstream. The 'Coanda effect' which makes the jets cling and attach to a solid surface tends to act on the plume-jet and makes it adhere to the wall surface. The plume grazing on the airframe wall is depicted through the adiabatic wall temperature contours around the jet trail in Fig.7. In the region of the jet trail from a distance 8.73D to 9.67D, the jet-flow adiabatic temperature **had observed** to be around 3000K. As the airframe material around the hot spot region is thin and made of Aluminum alloy, it is susceptible to get burned or melted.

Heat Conduction Analysis for the Plume-Body Interaction Zone

In order to assess the criticality of the aero-thermal problem, thermal analysis is made using CERANS and ATPC. Instead of using boundary layer method, an in-house developed and practiced, 'Isothermal method' [26] is used for evaluating the wall heat flux values. In this method, the heat transfer coefficient is assumed constant for determining the transient surface heat flux. This assumption is demonstrated to satisfy a wide range of thermal environments, provided the external flow condition does not vary significantly. However the Isothermal method requires a couple of flow simulations to be performed, one, an adiabatic flow simulation to obtain the adiabatic wall temperature and another, an isothermal cold wall simulation (say, $T_{\text{wall}}=300\text{K}$) for the same external flow conditions to obtain cold wall heat flux. The cold wall heat flux thus evaluated is used to find the heat transfer coefficient along with the adiabatic wall temperature using the definition of Stanton number. Using this heat transfer coefficient, the surface heat flux is estimated during temporal evolution of the heat conduction analysis for monitoring the temperature history of the airframe material.

Steps Involved in Thermal Analysis

The heat flux obtained using the isothermal method is imposed over the exposed top wall airframe material sur-

face for the one dimensional heat conduction analysis performed along the depth of the material using the ATPC code [24]. The bottom wall of the airframe material is considered as an adiabatic surface. At any given location on the airframe where the thermal health of the airframe material is required to be monitored (i.e., several point along the jet plume trail-body interaction zone downstream of the side jet nozzle as observed in Fig.7), a one dimensional equi-spaced grid consisting of 21 points along the depth of the airframe material is considered to solve the heat conduction equation for temporal evolution covering the entire duration of the flight. The material thermo-physical properties such as the density, thermal conductivity and the specific heat are specified as a polynomial function of temperature in the ATPC code. The output of ATPC code is presented as surface temperature history which can help determine the adequacy of the airframe design. The ATPC code is solved offline as it requires only the surface flow data such as heat flux and adiabatic wall temperature for performing the thermal analysis.

For the Aluminum alloy airframe (ALA-2014) with variable thicknesses from about 2.2 mm to 9.0 mm thickness, the temperature history at various axial locations ($X \sim 9D - 10D$) for the flight condition (Mach 0.54) are shown in Fig.8. It is observed that the temperature reaches the critical allowable limit from about 3 secs to 15 secs for the region from 9.06D to 9.33D. For locations beyond 9.33D, the temperature increase is benign and lies within allowable limit. Fig.8 shows the hot-spot zone falling between about 9D and 9.4D. The peak value of observed heat flux is about 120 W/cm^2 occurring at 9.07D location for the flight condition and about 140 W/cm^2 for the quiescent condition at the same location.

Design Change of Sustainer Nozzle from 'Scarf' to 'Conical'

CFD studies had clearly brought the vulnerability of airframe to high heat flux and high temperatures due to the grazing of plume exhausted from scarf sustainer nozzle. An alternative conical nozzle design is considered for the sustainer motor to avoid plume grazing over the airframe. In this design, the nozzle exit plane is perpendicular to the nozzle axis and in order to integrate the nozzle exit with the airframe, a bump-cum-dimple arrangement is made. The bump is due to the protrusion of nozzle out of the cylindrical body. The surface dimple is so chosen, that it should facilitate the jet plume to leave the nozzle exit-

plane and the dimple surface unobstructed throughout its period of operation.

CFD studies were also carried out for the flight vehicle with conical nozzle for various flow conditions, involving high angle of attack and as well as side-slip angles with sustainer jets on and off. The Mach contours around the scarf and conical nozzle exit is compared in Fig.9. It is clear from the figure that while the jet issuing out of the conical nozzle is travelling along in a straight path along the nozzle centre-line axis, without interfering any of the body components; the jet coming out from the scarf nozzle is gazing along the vehicle body (as discussed in Section - Thermal Problems Posed by the Scarf Nozzle). Also the adiabatic wall temperature near the dimple wall depicted had been found to be of the order of a benign $0.85T_{\infty}$. At the nozzle exit plane, the core pressure at the exit is slightly under-expanded ($1.2P_{\infty}$) and the exit Mach number is about 2.9. The exit temperature reached a value of 1700°C . This results indicate that the aero-thermal condition for the new 'Conical nozzle' is more benign than that of the 'Scarf nozzle'.

Fin Control Surface Deflection Characteristics with Conical Nozzle

Simulations are carried out for various fin deflections to evaluate the fin deflection characteristic of flight vehicle with conical nozzles. Control characteristic are evaluated for various fin deflections (same deflection angle for all panels) at two high angle of attack cases (16° and 20° respectively for jet-on and jet-off conditions). The variation of total normal force (C_N), pitching moment coefficients (C_m) and center of pressure (X_{cp}/D) with fin deflections for angles of attack of 16° and 20° are presented in Fig.10. It is observed that both C_N and C_m show linear variation with fin deflections and the slopes $C_{N\delta}$ and $C_{m\delta}$ appear to be similar for the two angles of attack. The control characteristics are found to increase by about 15% when the sustainer jets are on. As the fin deflection increases, X_{cp}/D moves rearward as expected. Also for any given fin deflection angle, as the angle of attack is increased, the X_{cp} moves rearward for negative fin deflection angles and it moves forward for positive fin deflection angles. It is interesting to observe that at $+20$ degrees fin deflections, X_{cp} for jet-on case is just about 0.1D behind the jet-off case. However for the -20 degrees fin deflections, the X_{cp} for jet-on case is about 0.5D ahead of the corresponding jet-off case.

Conclusions

The aerodynamic, aero-propulsion and aero-thermal characterization of flight vehicle configuration are carried out using the in-house developed CFD codes, CERANS and ATPC. Penetration of dual inclined supersonic jet into a subsonic crossflow is considered. 'Calorically Perfect Equivalent Specie' model is implemented in the CERANS code to model the jet-plume-free stream interaction. Exploration of flow variables obtained from the numerical simulation showed jet plume grazing and consequent severe heating of airframe due to the scarfing of sustainer nozzles. CFD analyses helped in design modification of the sustainer nozzle which resulted in the simple conical nozzle design that alleviated jet-plume interaction with the airframe. The control characteristics were found to increase by about 15% when the sustainer jets are on.

Acknowledgement

The authors express their sincere gratitude to the Director, Defence Research and Development Laboratory (DRDL) and Mr. K. V. Varaprasad, Scientist 'H', DRDL for their constant support, tireless reviews and encouragement. The support rendered by Scientists of Directorate of Aerodynamics, DRDL is sincerely acknowledged.

References

1. Dormieux, M. and Marsaa-Poey, R., "Numerical Assessment of Aerodynamic Interactions on Missiles with **tRansverse** Jets Control", Computational and Experimental Assessment of Jets in Cross Flow, AGARD CP 534, 1993, pp.30.1-30.11.
2. Cassel, L. A., "Applying Jet Interaction Technology", Journal of Spacecraft and Rockets, Vol.40, No.4, 2003, pp.523-537.
3. Srivastava, B., "Aerodynamic Performance of Supersonic Missile Body and Wing Tip Mounted Lateral Jets", Journal of Spacecraft and Rockets, Vol.35, No.3, 1998, pp.278-286.
4. Brandeis, J. and Gill, J., "Experimental Investigation of Super and Hypersonic Jet Interaction on Missile Configurations", Journal of Spacecraft and Rockets, Vol.35, No.3, 1998, pp.296-302.
5. Graham, M. J., Weinacht, P. and Brandeis, J., "Numerical Investigation of Supersonic Jet Inter-action



- for Finned Bodies", *Journal of Spacecraft and Rockets*, Vol.39, No.3, 2002, pp.376-383.
6. Margason, R. J., "Fifty Years of Jet in Cross Flow Research", *Computational and Experimental Assessment of Jets in Cross Flow*, AGARD CP 534, 1993, pp.1.1-1.41.
 7. Fric, T. F. and Roshko, A., "Vortical Structure in the Wake of a Transverse Jet", *Journal of Fluid Mechanics*, Vol.279, 1994, pp.1-47.
 8. Kelso, R. M., Lim, T. T. and Perry, A. E., "An Experimental Study of Round Jets in Crossflow", *Journal of Fluid Mechanics*, Vol.306, 1996, pp.111-144.
 9. McCann, G. J. and Bowersox, R. D. W., "Experimental Investigation of Supersonic Gaseous Injection into a Supersonic Freestream", *AIAA Journal*, Vol.34, No.2, 1996, pp.317-323.
 10. Aswin, G. and Debasis Chakraborty., "Numerical Simulation of Transverse Side Jet Interaction with Supersonic Free Stream", *Journal of Aerospace Sciences and Technologies*, Vol.14, 2010, pp.295-301.
 11. Saha, S., Sinha, P.K. and Debasis Chakraborty., "Numerical Prediction of Surface Heat Flux During Multiple Jets Firing for Missile Control", *Journal of Institute of Engineers (India), Series C*, Vol.94, Issue.1, January 2013, pp.85-91.
 12. Beresh, S. J., Henfling, J. F., Erven, R. J. and Spillers, R. W., "Turbulent Characteristics of a Transverse Supersonic Jet in a Subsonic Compressible Crossflow", *AIAA Journal*, Vol.43, No.11, 2005, pp.2385-2394.
 13. Beresh, S. J., Henfling, J. F., Erven, R. J. and Spillers, R. W., "Penetration of a Transverse Supersonic Jet into a Subsonic Compressible Crossflow", *AIAA Journal*, Vol.43, No.2, 2005, pp.379-389.
 14. Beresh, S. J., Henfling, J. F., Erven, R. J. and Spillers, R. W., "Vortex Structure Produced by a Laterally Inclined Supersonic Jet in Transonic Crossflow", *Journal of Propulsion and Power* Vol.23, No.2, March-April 2007, pp.353-363.
 15. Chocinski, D., Leblanc, R. and Hachemin J.V., "Experimental/Computational Investigation of Supersonic Jet in Subsonic Compressible Crossflow", *AIAA Paper No.97-0714*.
 16. Hojaji, M., Soltani, M.R. and Taeibi-Rahni, M., "New Visions in Experimental Investigations of a Supersonic Under-Expanded Jet into a High Subsonic Crossflow", *Proc. IMechE*, Vol.224, Part G: *Journal of Aerospace Engineering*, March 2010, pp.1069-1080.
 17. Arunajatesan, S., "Evaluation of Two-Equation RANS Models for Simulation of Jet-in-Crossflow Problems", *AIAA Paper 2012-1199*.
 18. X. Chai and Mahesh, K., "Simulations of High Speed Turbulent Jets in Crossflow", *AIAA Paper No.2011-650*.
 19. Balasubramanian, R. and Anandhanarayanan, K., "Numerical Simulation of Low Speed Flows Using a Compressible Viscous Flow Solver", *Proceedings of Marine Hydrodynamics Conference, MAHY-06, NSTL, Vizag, India, January 2006*.
 20. Balasubramanian, R., Anandhanarayanan, K. and Balakrishnan, N., "Development of a 3-D Compressible Reynolds Averaged Navier-Stokes solver", *Proceedings of European Congress on Computational Methods in Applied Sciences and Engineering, ECCOMAS 2004, Jyvaskyla, Finland, 24-28, July 2004*.
 21. Balasubramanian, R., Anandhanarayanan, K., Krishnamurthy, R. and Debasis Chakraborty., "Numerical Simulation of Stage Jettisoning of a Two-Stage Rocket with Different Separation Distances", *Journal of Institution of Engineers (India), Series-C*, Vol.93(4), 2012, pp.345-350.
 22. Balasubramanian, R. and Anandhanarayanan, K., "Viscous Computations for Complex Flight Vehicles using CERANS with Wall Function", *CFD Journal*, Vol.16. No.4, 2008, pp-386-390.
 23. ICEM-CFD, Release 11.0: Installation and Overview, July 7th 2007.
 24. Kim, S. S., Kim, C., Rho, O. H. and Hong, S.K., "Cures for shock instability: Development of a

Shock-Stable Roe Scheme", Journal of Computational Physics, Vol.185, 2003, pp.342-374.

25. Spalart, P. R. and Allmaras, S. R., "A One-Equation Turbulence Model for Aerodynamic Flows", AIAA Paper 92-0439, 1992.
26. Les Hall., Applebaum, M. P. and Eppard, W.M., "Multi-Species Effects for Plume Modeling on Launch Vehicle Systems", AIAA Paper No.2011-1053.
27. Balasubramanian, R., Anandhanarayanan, K., Krishnamurthy, R. and Debasis Chakraborty., "A High Fidelity Kinetic Heating Analysis Suite For High Speed Flight Vehicles", Proceedings of National Seminar on Expanding Frontiers in Aerospace Tech-

nologies - Challenges and Opportunities, at 26th National Convention of Aerospace Engineers, Hyderabad, 24-25 November, 2012, pp.198-202.

28. Cowart, K. and Olds, J., "TCAT - A Tool for Automated Thermal Protection System Design", AIAA Paper 2000-5265.
29. Chandra Murty, M.S.R., Bhandarkar, A.V., Sinha, P.K., and Debasis Chakraborty., "Application of CFD Based Methods in the Kinetic Heating Analysis of a Air-to-Air Aerospace Vehicle", Proceedings of National Seminar on Expanding Frontiers in Aerospace Technologies - Challenges and Opportunities, at 26th National Convention of Aerospace Engineers, Hyderabad, 24-25 November, 2012, pp.187-192.

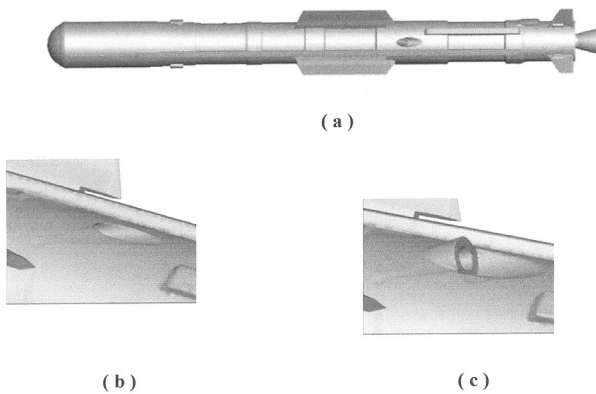


Fig.1 Flight Vehicle Configuration (a) Full Vehicle (b) With Scarf Nozzle (c) With Conical Nozzle

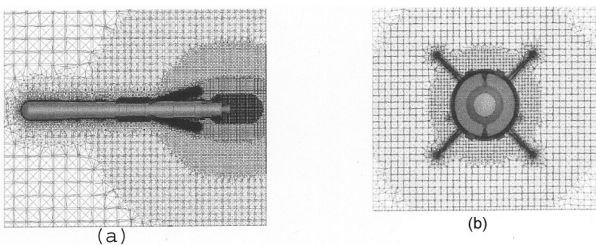


Fig.2 Computational Grid (a) In Pitch Plane (b) At Cross Section

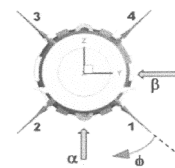


Fig.3 Numbering and Flow angles (Rear View)

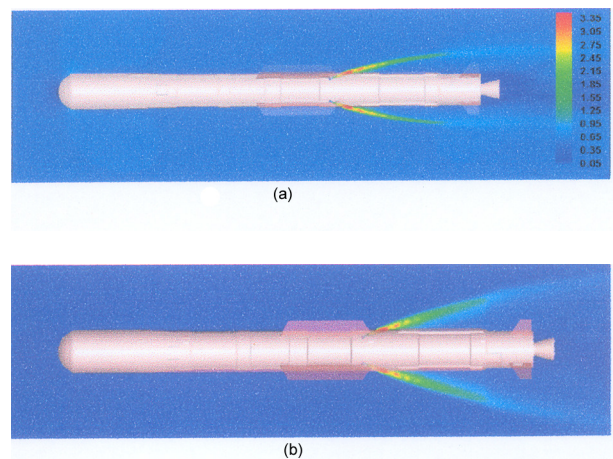


Fig.4 Mach Contours (Scarf Nozzle) (a) $M = 0.54, \alpha = 4^\circ$ (b) $M = 0.1, \alpha = 4^\circ$

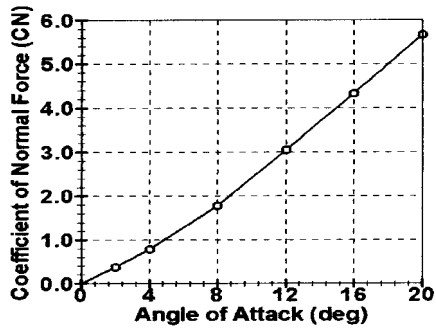


Fig.5 C_N Vs α (Mach 0.54)

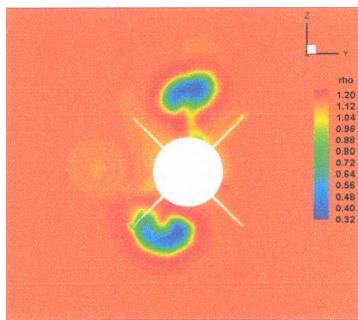


Fig.6 Jet Impingement Over a Fin at Side Slip (View at Fin Cross Section)

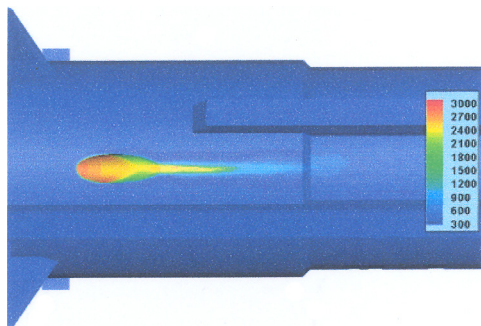


Fig.7 Adiabatic Wall Temperature Contours Around the Trail of Jet

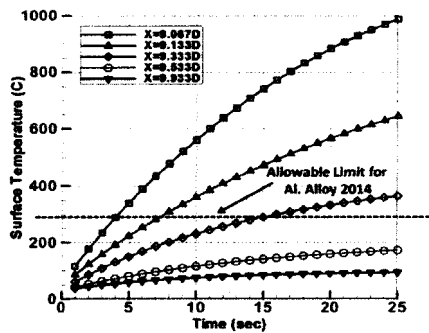


Fig.8 Temperature History at Various Axial Position for Scarf Nozzle at $M_\infty = 0.54$

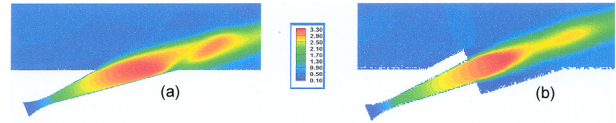


Fig.9 Mach Contours Around Nozzle Exit Region (a) Scarf Nozzle (b) Conical Nozzle

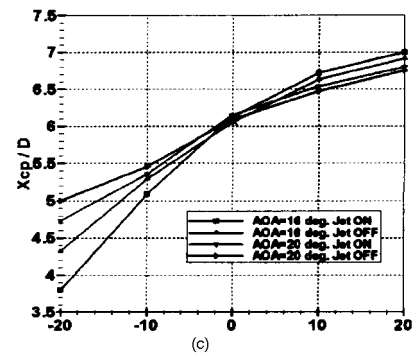
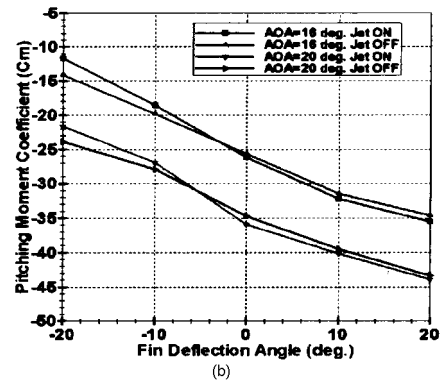
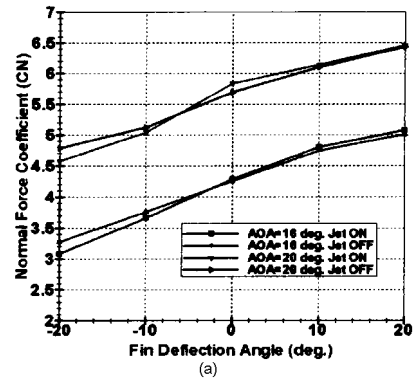


Fig.10 Variation of (a) C_N (b) C_m and (c) X_{cp}/D with Fin Deflection